Air Drying of Milk Droplet under Constant and Time-Dependent Conditions

Xiao Dong Chen and Sean Xu Qi Lin
Food and Bioproduct Processing Cluster, Dept. of Chemical & Materials Engineering, The University of Auckland, Auckland, New Zealand

DOI 10.1002/aic.10449
Published online April 11, 2005 in Wiley InterScience (www.interscience.wiley.com).

Spray drying is the prime process for many years for manufacturing food powders. Dairy powders are one of the main products consumed worldwide. There has been a stream of studies published previously on both modeling the drying characteristics of a single milk droplet and the dryer wide simulations incorporating computational fluid dynamics (CFD). In CFD simulations, large numbers of particles of different sizes need be tracked to represent the size distribution; it is desirable to have an accurate yet simple model for drying of a single droplet, which does not require partial differential equation. Here for the first time, two such models are validated. One model is of the characteristic drying rate curve approach and the other (new) model is of the reaction engineering approach. The model predictions are compared against a very wide range of experimental results including isothermal and time-varying temperature conditions. © 2005 American Institute of Chemical Engineers *AIChE J,* 51: 1790–1799, 2005
Keywords: drying of milk, droplet drying kinetics, glass filament method, chemical reaction engineering approach, drying characteristic rate curve

Introduction

Drying is a key final process during the manufacture of food products. It is a traditional means of preservation, although food—which is one of the most complex materials in natural form—and the fundamental understanding of food drying has not been fully established.[1,2] Spray drying is the prime process for making powdered products. Many studies have been published on the modeling of drying but the differences among the model formulations can be considerable.[3] Often, the proposed models can be compared only with rather specific sets of data. Accurate data on drying of milk droplets and other food suspensions for a wider range of experimental conditions, which can be used to establish mathematical models for spray drying, are still very limited.

More recently, for milk products, Lin and Chen[4] established a comprehensive lab system to investigate the drying behavior of single droplets and the equilibrium isotherms for samples having high water content. They obtained extensive data on isothermal drying conditions[4] and in this paper the results of variable drying conditions are also presented. Herein, an attempt has been made to examine two significant models in a more comprehensive manner. One is the previously established characteristic drying rate model and one is a more recent reaction engineering model. The reaction engineering model has not been rigorously tested using comprehensive data sets such as those in the current work. Both isothermal and variable drying experiments were used to validate the models.

A Brief Review of Drying Models

For the prediction of single droplet drying, there are generally four types of approaches to formulating drying models:

(1) The *comprehensive transport phenomena* approach, using coupled heat and mass diffusion equations.[5-7]

(2) The *characteristic drying rate curve* (CDRC) approach, which divides the drying process into different drying stages, such as constant drying period and falling rate period(s).[8]

(3) The *reaction engineering approach* (REA), that is, as-

Correspondence concerning this article should be addressed to X. D. Chen at d.chen@auckland.ac.nz.

suming drying is a competitive process between "evaporation reaction " and "condensation reaction." [3]

(4) The *empirical models* obtained entirely by regression methods to obtain the explicit time-dependency functions.

The two effective approaches—CDRC and REA—are the focus of the current work and the other approaches, either those having partial differential equations or those of overly simplistic models, are not considered herein. Both the CDRC and the REA models have the advantage in reducing computational time in future computational fluid dynamics (CFD) approach to simulating spray drying systems because they do not involve computations for the spatial concentration distribution within a droplet/particle being dried.

The characteristic drying rate curve approach

The CDRC approach assumes that for a free moisture content there is a corresponding specific drying rate relative to the unhindered drying (evaporation) rate.[8] The relative drying rate is defined as

$$f = \frac{N_v}{\hat{N}_v} \tag{1}$$

where N_v is the drying rate at any stage, $\hat{N}_v$ is the drying rate in the first drying period (which is usually the constant rate or the unhindered drying rate period). The characteristic moisture content is defined as

$$\phi = \frac{X - X_b}{X_{cr} - X_b} \tag{2}$$

where X is the average water content on a dry basis, X_b is the equilibrium moisture content corresponding to the environmental condition for drying, and X_{cr} is the critical moisture content (which makes the transition from the constant rate period to the first falling rate period). The relative drying rate f or the shape of the drying rate curve for a given material is taken to be a unique function of the characteristic moisture content ϕ according to the hypothesis of characteristic drying rate curve theory.

Langrish and Kockel[8] used the initial water content X_0 to replace X_{cr} for the materials that have no constant drying rate period and assumed the relative drying rate f is proportional to the free moisture content $(X - X_b)$ (linear falling rate curve). Thus the drying rate can be written in the following form

$$-\frac{dX}{dt} = (X - X_b)[\beta_2(\rho_{v,s} - \rho_{v,b})] \tag{3}$$

where X is the mean water content on a dry basis. Because the vapor pressure driving force is virtually proportional to the wet bulb depression,[8] Eq. 3 can be rewritten in the following form

$$-\frac{dX}{dt} \cong (X - X_b)[\beta_3(T_b - T_{wb})] \tag{4}$$

where t is time; T_b and T_{wb} are bulk and wet bulb temperature of the drying air, respectively; and the coefficient β_3 is equal to the external heat transfer coefficient divided by the product of the mass of dry solid per unit surface m_s/A, the initial free moisture content $(X_0 - X_b)$, and the latent heat of vaporization ΔH_l

$$\beta_3 = \frac{h}{(m_s/A)(X_0 - X_b)\Delta H_l} \tag{5}$$

where h is the external heat transfer coefficient; m_s is the mass of the solids in one droplet/particle; A is the surface area of the droplet; X_0 and X_b are droplet initial moisture content and equilibrium moisture content, respectively; and ΔH_l is the latent heat of water vaporization.

The energy balance used for the model is given in the following form

$$mC_{p,d}\frac{dT_d}{dt} = hA(T_b - T_d) + \Delta H_l m_s \frac{dX}{dt} \tag{6}$$

where $C_{p,d}$ is the specific heat capacity of the droplet, T_d is droplet temperature (assumed to be uniform throughout the droplet), T_b is drying air temperature, and m is the droplet mass.

The heat transfer coefficient h and the mass transfer coefficient h_m are obtained from the established correlations such as the Ranz–Marshall correlation,[10] which has the following form

$$\mathrm{Nu} = 2 + 0.60\mathrm{Re}^{1/2}\mathrm{Pr}^{1/3} \tag{7}$$

$$\mathrm{Sh} = 2 + 0.60\mathrm{Re}^{1/2}\mathrm{Sc}^{1/3} \tag{8}$$

It has been shown by Lin and Chen[4] that the Ranz–Marshall correlation overestimates the mass transfer rate. The lab work carried out by the same authors have yielded the more appropriate correlation for the lab conditions investigated here. The new correlations (Eqs. 15 and 16) have also been used to examine the CDRC method.

The reaction engineering approach

When the droplet is being dried, the drying rate can be expressed in the following form

$$\frac{dm}{dt} = -h_m A(\rho_{v,s} - \rho_{v,b}) \tag{9}$$

where $\rho_{v,s}$ is the vapor concentration at the particle–gas interface and $\rho_{v,b}$ is the bulk vapor concentration. However, $\rho_{v,s}$ is an unknown parameter that is time dependent during the drying process as a result of the increasing solid content at the surface. It is known that $\rho_{v,s}$ can be related to the saturation water vapor concentration as follows

$$\rho_{v,s} = \psi\rho_{v,sat}(T_s) \tag{10}$$

where ψ is a fractionality coefficient relative to the moisture content of the dried product at the interface and T_s is the interface temperature. The interface temperature is approximately the droplet temperature T_d if the Biot number is small

enough. In effect, ψ is the relative humidity at the interface of the droplet/particle and the drying air.

The reaction engineering approach assumes that evaporation is an "activation " process having to overcome an "energy barrier," whereas condensation or adsorption is not. It uses a simple relationship to express ψ (approximately) as a function of water content and temperature as follows[3,12]

$$\psi = \exp\left(-\frac{\Delta E_v}{RT_d}\right) \tag{11}$$

where ΔE_v is essentially a "correction factor " of the apparent activation energy for drying because of the increasing difficulty of removing water at low moisture content levels. It is expected that Eq. 11 is unity when the droplet/particle surface is saturated with water vapor. In other words, this correction factor (ΔE_v) would be zero when excess water is present at the surface.

By combining Eqs. 10 and 11 and substituting them into Eq. 9, one obtains

$$\frac{dm}{dt} = -h_m A\left[\rho_{v,sat}\exp\left(-\frac{\Delta E_v}{RT_d}\right) - \rho_{v,b}\right] \tag{12}$$

From Eqs. 10 and 11, the apparent activation energy for drying can be written in the following form

$$\Delta E_v = -RT\ln\left(\frac{\rho_{v,s}}{\rho_{v,sat}}\right) \tag{13}$$

Therefore, the apparent activation energy reflects the vapor concentration depression $\rho_{v,s}/\rho_{v,sat}$ of the dried material as the water content decreases. Equation 13 can be obtained through the drying experiments and ΔE_v can then be plotted against the mean water content of the droplet/particle of concern.

For a drying process, the REA model assumes that the relationships between the apparent activation energy vs. moisture content as the characteristic properties of the individual material under various drying conditions. This means that the vapor concentration at the particle–gas interface may be calculated from the apparent activation energy ΔE_v. The drying rate of the moist solid would then be solved using Eq. 9.

The heat transfer coefficient h and the mass transfer coefficient h_m may be calculated from Eqs. 7 and 8 or obtained from the other established correlations.[4,11]

The drying surface areas for milk droplets have been obtained experimentally.[4,12] The energy balance equation used for the model is the same as Eq. 6.

Experimental

The details of the apparatus and the experimental procedures have been described in detail most recently by Lin and Chen.[4] The glass-filament method has been adopted, that is, the droplet weight was measured by recording the deflection of the glass filament as long as the values are corrected for the corresponding drag forces. The air-flow effect on the measurement can be corrected through calibration with respect to the drag it causes.[4]

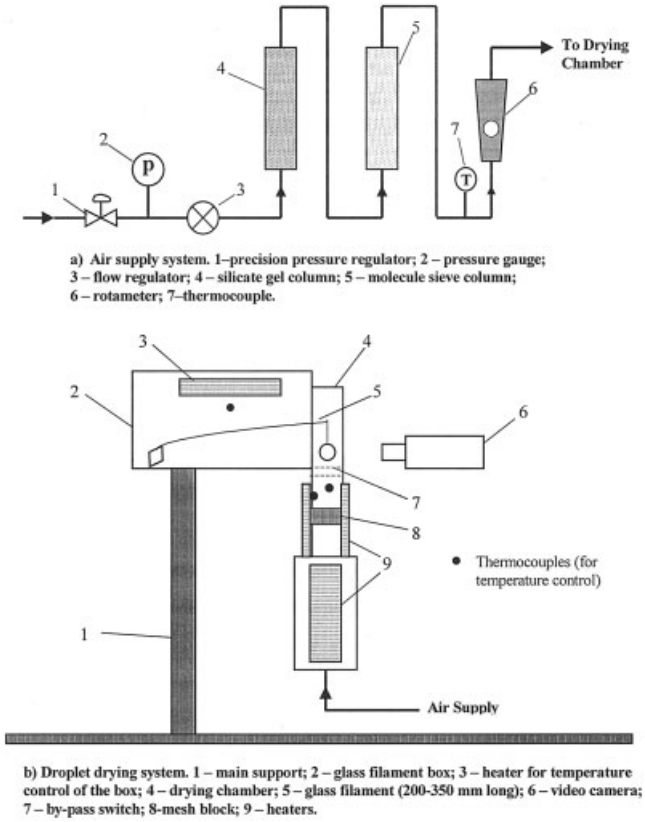

a) Air supply system. 1–precision pressure regulator; 2 – pressure gauge; 3 – flow regulator; 4 – silicate gel column; 5 – molecule sieve column; 6 – rotameter; 7–thermocouple.

b) Droplet drying system. 1 – main support; 2 – glass filament box; 3 – heater for temperature control of the box; 4 – drying chamber; 5 – glass filament (200-350 mm long); 6 – video camera; 7 – by-pass switch; 8-mesh block; 9 – heaters.

Figure 1. Present experimental setup.

In this study, a wider range of data has been obtained, including the temperature/time-varying experiments.

A brief summary of the experimental setup and method is as follows: The droplet to be dried is suspended in a uniform, preconditioned (temperature and humidity) air stream by a glass filament. The thin tip section of the glass filament is 30–100 μm in diameter. At the end of the thin tip section there is a glass knob (100–220 μm) coated with Teflon®, which is used for the suspension of the droplet. The cross-sectional area of the drying tunnel is 29.97 $\times$ 29.97 ($\pm$0.02) mm. The deflection of the glass filament and droplet diameter change during drying is recorded continuously using a standard video camera (Panasonic M3000) fitted with four close-up lenses (Jessop +4). The recorded images are then transferred to a digital signal using a video capture card (Pinnacle DC 10 Plus) and analyzed by image analysis software (UTHSCSA, Image Tool). The magnification of the video camera system is 50 $\times$ at a resolution of 0.8 mm. The system is schematically shown in Figure 1.

The temperature/time history of the droplet is measured separately from that of the weight measurements, for the same droplet size and composition under the same drying conditions (see Figure 2). The measurement device consists of a calibrated thermocouple (13 or 24 μm in diameter).

The repeatability of the weight loss of the experiment was $\pm$0.01 mg and the accuracy of weight measurements was 0.05 mg. The droplet temperature and diameter were also measured experimentally. The accuracy of the temperature measurement was believed to be within 0.1°C.[4]

For the droplet drying in constant drying conditions, the

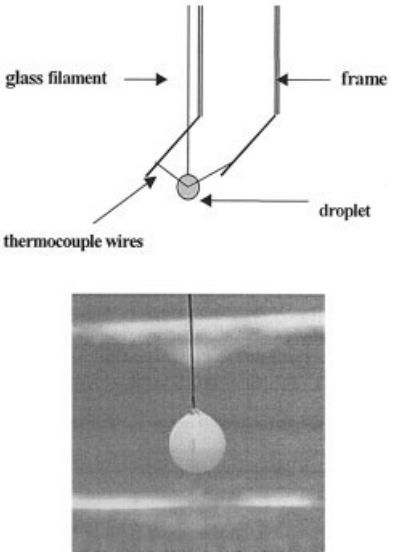

Figure 2. Droplet temperature measurement.

drying tunnel provides constant temperature and humidity. The drag forces were measured at a constant experimental temperature and corrected for the droplet weight calculation.

The constant (isothermal) drying conditions under which the droplets were dried were as follows:

- Drying air temperature: 67–110°C
- Drying air velocity: 0.45–1.00 m s^{-1} (Re = 30–80)
- Initial droplet diameter: 1.45 mm
- Initial solids concentration: 20.0 and 30.0 wt %
- Drying air humidity: 0.0001 kg kg^{-1}

For the droplet drying under varying temperature-time conditions, the drying air humidity was kept at 0.0001 kg kg^{-1} and the drying air temperature was allowed to decrease by simply stop heating as soon as drying started. During this drying process, the drying tunnel temperature uniformity at the cross-section of the droplet drying level was within 2.0°C. The drying tunnel temperature was thus varied and its repeatability has been assessed and the average difference of the two experiments under the same condition was within 0.4°C. The temperature measurement device was a calibrated thermocouple 24 μm in diameter (accuracy of 0.1°C). For the temperature/time-varying conditions, the drag forces were measured at different temperatures and corrected for the droplet weight calculation.

The conditions for the temperature/time-varying experiments were as follows:

- Initial drying air temperature: 91.4 and 113.4°C
- Drying air flow rate: 30.0 standard liters per minute (SLPM)
- Initial droplet diameter: about 1.42 mm
- Initial solids concentration: 20.0 and 30.0 wt %
- Drying air humidity: 0.0001 kg kg^{-1}

The above experiments were performed with the aim of validating the two models presented herein under temperature/time-varying conditions. In the past, no such experiments were conducted. Previous studies were all carried out under constant drying conditions for the droplets.

The liquid droplets were prepared by reconstituting milk powders, which were purchased from the local market, and their compositions are given in Table 1.

Determining the Activation Energy Experimentally

To obtain ΔE_v experimentally, at different average water contents, Eq. 12 can be rewritten as the following form:

$$\Delta E_v = -RT_d \ln\left(\frac{-\frac{dm}{dt}\frac{1}{h_m A} + \rho_{v,b}}{\rho_{v,sat}}\right) \tag{14}$$

Here, dm/dt was obtained from the experimental droplet weight loss curve. The droplet evaporation areas were also measured experimentally, by using a previously discussed method.[4,16] The saturated vapor concentration at the particle–gas interface was calculated in terms of the droplet temperature, which was also measured experimentally at the center of the droplet. Finally, the mass and heat transfer coefficients were calculated by the following correlations, obtained in this study for the conditions examined.[4] The lower coefficients in the mass transfer correlation (Eq. 16) for the experiments conducted here, compared with those of the Ranz–Marshall correlation (Eq. 8), have been explained by Chen[13]

$$\mathrm{Nu} = 2.04 + 0.62\mathrm{Re}^{1/2}\mathrm{Pr}^{1/3} \tag{15}$$

$$\mathrm{Sh} = 1.63 + 0.54\mathrm{Re}^{1/2}\mathrm{Sc}^{1/3} \tag{16}$$

Figures 3 and 4 show the apparent and the normalized activation energy of skim milk drying at different drying conditions, respectively. One can see that the scattering of the data points is not extensive. For the droplet drying at different ambient conditions, the activation energy ΔE_v vs. free moisture content $(X - X_b)$ may be normalized to a 0-to-1 scale according to the original idea[3]

$$\frac{\Delta E_v}{\Delta E_{v,b}} = g(X - X_b) \tag{17}$$

where $\Delta E_{v,b}$ is "equilibrium " activation energy, which can be calculated by Eq. 13 using the bulk fluid condition. The equilibrium vapor concentration $\rho_{v,b}$ is related to the corresponding equilibrium water content of the milk at different temperatures through the desorption isotherm [that is, the GAB (Guggenheim–Anderson–de Boer) equation][14]

$$X_e = \frac{Ckm_0 a_w}{(1 - ka_w)(1 - ka_w + Cka_w)} \tag{18a}$$

where X_e is the equilibrium moisture content (the X_e corresponding to $\rho_{v,b}$), a_w is the water activity [the relative humid-

Table 1. Composition (wt %) of Skim and Whole Milk Powders before Being Reconstituted in Water

Component	Skim Milk Powder	Whole Milk Powder
Fat	0.6	26.5
Total protein	36.5	28
Lactose	49.8	36.8
Mineral	9.3	5.9
Moisture	3.8	2.8

ity = $\rho_{v,b}/\rho_{v,sat}(T_b)$], m_0 is the monolayer moisture content, and C and k are temperature-dependent constants, expressed as

$$C = C_0 \exp\left(\frac{\Delta H_1}{RT}\right) \tag{18b}$$

$$k = k_0 \exp\left(\frac{\Delta H_2}{RT}\right) \tag{18c}$$

The coefficients in Eq. 18 were obtained through experimentation for relative humidity up to 100% by the same authors.[14] The monolayer moisture contents (m_0) of the skim milk powder and whole milk powder, which were 0.06156 and 0.04277 kg/kg, respectively. The values of C (indirect regression) for skim milk and whole milk decreased when the temperature was increased and were related to the temperature (ΔH_1 = 24,831 J/mol, C_0 = 0.001645, R^2 = 0.9999 for skim milk; ΔH_1 = 10,485 J/mol, C_0 = 0.1925, R^2 = 0.998 for whole milk powder). The values of k (indirect regression) increased with increasing temperature and were related to the temperature (ΔH_2 = −5118 J/mol, k_0 = 5.710, R^2 = 0.996 for skim milk; ΔH_2 = −3215 J/mol, k_0 = 2.960, R^2 = 0.999 for whole milk).

The droplet temperature during drying can be assumed to be uniform throughout the droplet and measured by a fine thermocouple, as mentioned earlier. This, according to the conventional theory, requires a small Biot (Bi) number[15,16]

$$\text{Bi} = \frac{hd}{2k} < 0.1 \tag{19}$$

In this experiment, the Bi number was estimated between 0.1 and 0.25. Because there is evaporation on or inside the droplet/particle during drying, the temperature difference within the droplet is actually smaller than that estimated using the conventional Bi number definition.[15] Therefore, the temperature gradient in the droplet/particle is assumed to be negligible.

In terms of Eq. 14, the activation energy was calculated from the drying curves (weight loss vs. time), obtained experimentally. Figures 3 and 4, respectively, show the original activation energy and the normalized activation energy vs. average moisture content difference ($X - X_b$) for skim milk. The same set of data was obtained for whole milk (results not shown). The experiments were conducted at different drying air temperatures and velocities as well as different initial concentrations as mentioned above. It can be seen that the normalized activation energy and the average moisture content difference may be approximated as being unique and independent of the drying air conditions. The resulting correlations of the normalized activation energy vs. moisture content difference for skim and whole milk are as follows:

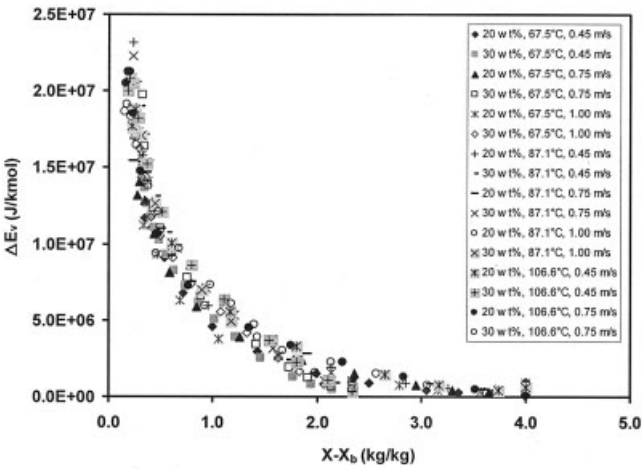

Figure 3. Relationship between the normalized activation energy and free moisture content during drying for skim milk.

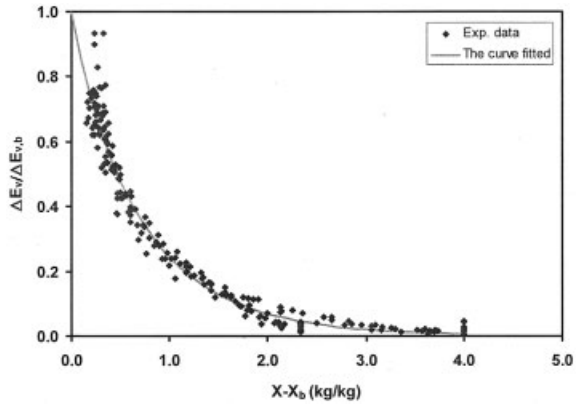

Figure 4. Comparison of the experimental data and predictions given by the REA model for 20 wt % skim milk drying at T_b = 67.5°C, v_b = 0.45 m/s, and H = 0.0001 kg/kg.

Droplet initial weight = 1.727×10^{-6} kg.

Skim Milk

$$\frac{\Delta E_v}{\Delta E_{v,b}} = 0.998 \exp[-1.405(X - X_b)^{0.930}] \tag{20}$$

Whole Milk

$$\frac{\Delta E_v}{\Delta E_{v,b}} = 0.957 \exp[-1.291(X - X_b)^{0.934}] \tag{21}$$

Unified

$$\frac{\Delta E_v}{\Delta E_{v,b}} = 0.978 \exp[-1.348(X - X_b)^{0.932}] \tag{22}$$

Equations 20 and 21 are the individual correlation for skim and whole milk drying, respectively. The practical situation is that fairly similar operation conditions are used for drying of skim and whole milk in the dairy industry. On observing Eqs. 20 and 21 one can see that the normalized equations may be made identical and the errors incurred might not be large (this was the case; results not shown). Equation 22 is thus the unified correlation for both milk types. Furthermore, one may set the preexponential factor to be unity. This has been seen (results not shown here) to yield small differences (slightly poorer fits overall obtained) and this may be attributed to the experimental

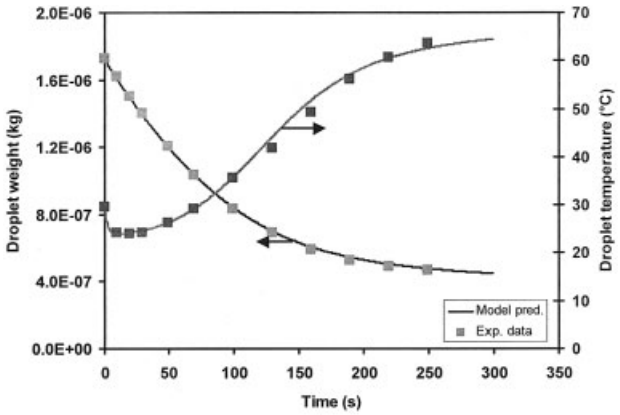

Figure 5. Apparent activation energy of skim milk drying under different constant drying conditions.

inaccuracy at very low drying rates toward the end of the drying process. The activation energy approaches zero as free moisture content increases and, gradually, the drying process becomes the evaporation of pure water. When the moisture content decreases toward the corresponding equilibrium content, the normalized activation energy approaches unity, that is, ΔE_v equals the "equilibrium " activation energy. This means that the droplet reaches the equilibrium moisture content and there is no further drying. For the intermediate moisture content, the normalized activation energy reflects the vapor concentration depression from vapor with respect to the case of pure water. Although not observed in previous studies,[3] even the direct plots of ΔE_v vs. $(X - X_b)$ are characterized by only slight scattering. As such, for the first time, it may even be possible to correlate ΔE_v vs. $(X - X_b)$ for both milk types without the $\Delta E_{v,b}$ normalization. The unified correlation for ΔE_v is given as

$$\Delta E_v = 2.4254 \times 10^7 \exp[-1.348(X - X_b)^{0.932}] \quad (23)$$

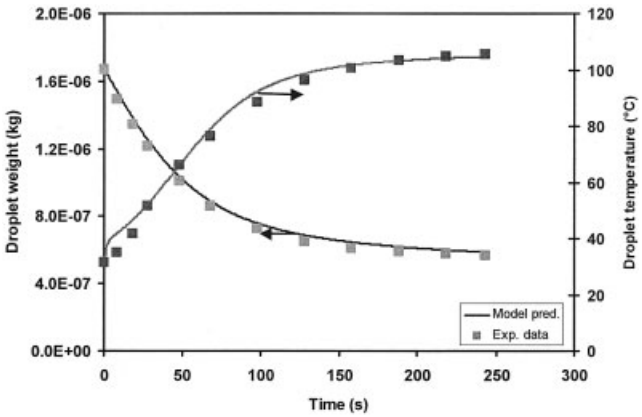

Figure 6. Comparison of the experimental data and predictions given by the REA model for 30 wt % whole milk drying at T_b = 106.6°C, v_b = 0.75 m/s, and H = 0.0001 kg/kg.

Droplet initial weight = 1.668×10^{-6} kg.

Table 2. Drying Conditions That Were Used in Model Predictions under Constant Drying Conditions

Drying Air Temperature (°C)	Drying Air Velocity (m/s)		
	0.45	0.78	1.00
67.5	*, **	*, **	*, **
87.1	*, **	*, **	*, **
106.6	*, **	*, **	*, **

* 20.0 and 30.0 wt % skim milk tested.
** 20.0 and 30.0 wt % whole milk tested.

For a direct application of the above equation, however, caution is required.

Results and Discussion

Droplet drying modeling under constant drying conditions

The simulations were conducted for the same conditions as in the experimental conditions to see how good the two models behave. Modeling with the REA approach was made following the finite-difference (explicit) method. The procedures are given as follows:

(1) The droplet weight, temperature, diameter, and moisture content were given as initial values (the same as the experimental values).

(2) The film temperature was calculated. Then the Nusselt (Nu) and Sherwood (Sh) numbers were calculated using Eqs. 15 and 16, thus allowing the heat and mass transfer coefficient to be determined.

(3) The saturated vapor concentration was determined at the droplet temperature and the activation energy was calculated using Eq. 20 or 21 for skim or whole milk, respectively. Then the droplet surface vapor concentration was calculated using Eqs. 10 and 11.

(4) The drying rate dm/dt was calculated using Eq. 9 and the rate of the droplet temperature change dT/dt was determined using Eq. 6.

(5) For the next time step, the droplet weight and temperature (here the time step was chosen to be 0.5 s; a smaller time step of 0.25 s scarcely altered the results) was calculated using the previous value and rate change. The droplet diameter change was calculated using an experimental correlation.[17]

(6) The new values of the droplet's weight, temperature, diameter, and moisture content were then obtained at step 5 and a new calculation cycle was repeated from step 2 to step 5 and so on.

Figures 5 and 6 present typical comparisons of the experimental and the predicted droplet temperatures and droplet weights during drying using the REA model for both skim and whole milk. The predictions were carried out under all the experimental conditions listed in Table 2. The average absolute difference between the experimental and the predicted values was 1.1% (for skim milk) and 1.6% (for whole milk) of the initial droplet weight for the droplet weight loss and 1.6°C (for skim milk) and 2.0°C (for whole milk) with respect to the droplet temperature.

Generally, the predictions are in very good agreements with the experimental data under all the conditions tested. The REA model predicts the droplet-drying trend in detail. For the temperature prediction, the agreement in the constant drying tem-

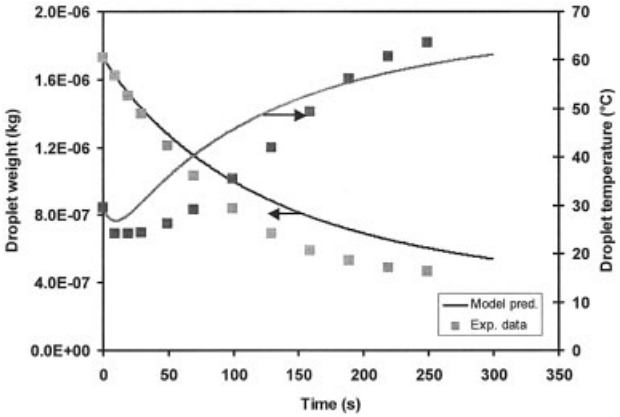

Figure 7. Comparison of the experimental data and predictions given by the CDRC model for 20 wt % skim milk drying at T_b = 67.5°C, v_b = 0.45 m/s, and H = 0.0001 kg/kg.

Droplet initial weight = 1.727×10^{-6} kg.

perature period of the 30.0 wt % milk between experimental and prediction was less desirable, which could be explained by the following: When the droplet began to dry, for example, a milk droplet with 30.0 wt % initial solids concentration, the surface of the droplet might be filled with free moisture. The activation energy would be very close to zero. However, the REA approach yielded a mother curve, which may not allow for this proximity to zero. The activation energy might thus be overestimated for the very beginning of the drying process. Such overprediction happened in the first 10 to 20 s. Despite this, the maximum temperature difference between experiment and prediction was still <3°C.

The CDRC model predictions under the same conditions as above were also made for comparison. In this simulation, the droplet diameter change was obtained from the same experimental correlation (the same as activation energy model), which is an advance from the previously used perfect shrinking model, which assumes that the drop size reduction is solely a result of water volume reduction. Figure 7 shows a typical result simulated using the CDRC for 20 wt % solids milks. The model predicts much better for the 30 wt % milks (similar to that using the REA model; results not shown here). The predictions were carried out for the same experimental data sets as those used for the REA model. The average absolute difference between experimental and prediction was 3.9% (for skim milk) and 2.9% (for whole milk) of the initial droplet weight for the droplet weight loss, and 3.6°C (for skim milk) and 3.4°C (for whole milk) for the droplet temperature prediction. Greater

Table 3. Average Absolute Differences between the Experimental Data and Predictions by Either REA or CDRC Approach under Constant Drying Conditions

	REA		CDRC	
	Temperature (°C)	Weight (%)	Temperature (°C)	Weight (%)
Skim milk	1.6	1.1	3.6	3.8
Whole milk	2.0	1.6	3.4	2.9

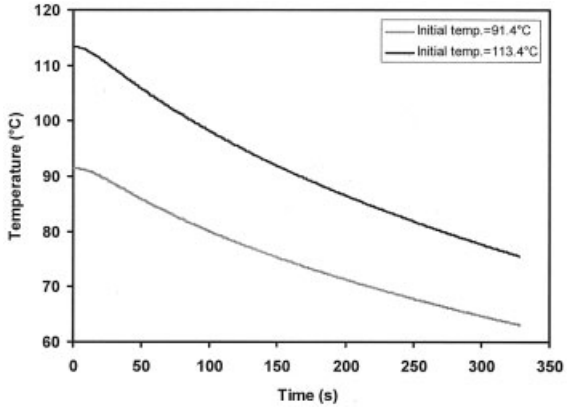

Figure 8. Drying tunnel temperature changes during time-dependent drying conditions.

discrepancies have been found, although there is no doubt that the CDRC model, simple as it is, predicts the trends well.

A summary of the average absolute differences between the experimental data and the predictions by the REA and the CDRC model is provided in Table 3.

Modeling droplet drying under time-dependent drying conditions

As mentioned earlier, the experimental work was carried out in this study using the glass-filament method[4] under varying drying conditions. The drying tunnel temperature changes are shown in Figure 8. The simulations were conducted using both of the above models under the same experimental conditions. The modeling procedures were similar to those under constant drying conditions, except that the drying temperature change was taken into account.

Figures 9 and 10 present the comparisons of the experimental and the predicted droplet temperature and weight loss during (varying conditions) drying by the REA model for the skim milks. These are typical results of the predictions and experimental results. The predictions were also carried out under all the experimental conditions listed in Table 4. The average

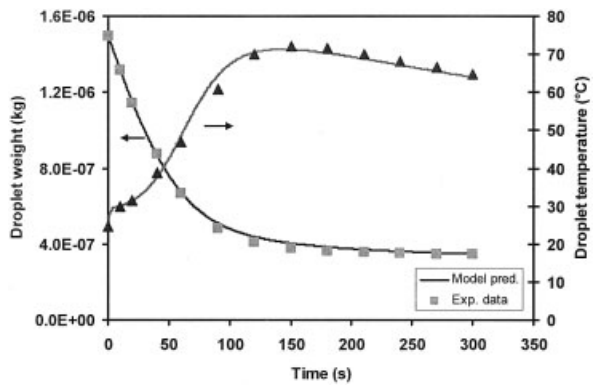

Figure 9. Comparison of the experimental data and predictions given by the REA model for 20 wt % skim milk under time-dependent drying conditions.

T_i = 91.4°C, v_b = 30 SLPM, H = 0.0001 kg/kg, and droplet initial weight = 1.494×10^{-6} kg.

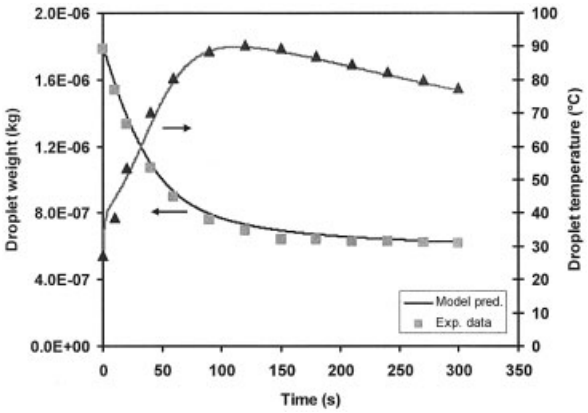

Figure 10. Comparison of the experimental data and predictions given by the REA model for 30 wt % skim milk under time-dependent drying conditions.

T_i = 113.4°C, v_b = 30 SLPM, H = 0.0001 kg/kg and droplet initial weight = 1.785×10^{-6} kg.

absolute differences between the experimental and the predicted values were 1.6% (for skim milk) and 1.1% (for whole milk) of the initial droplet weight for the droplet weight loss and 2.0°C (for skim milk) and 2.0°C (for whole milk) for the droplet temperature prediction, respectively.

The above experimental data set was also used to test the CDRC model. The same droplet diameter change correlation was used as that used in the REA approach. The predictions were also carried out for all the experimental conditions listed in Table 4. The average absolute differences between experimental and prediction were 3.8% (for skim milk) and 3.0% (for whole milk) of the initial droplet weight for the droplet weight loss and 4.3°C (for skim milk) and 2.1°C (for whole milk), respectively (plots not shown).

A summary of the average absolute differences between the experimental data and the predictions by the REA or the CDRC approach under the time-dependent drying conditions is provided in Table 5.

Discussion on REA and CDRC Models

From Tables 3 and 5, it was found that the differences between the experimental data and the predictions made by the REA model are smaller than those of the CDRC approach.

Figure 11 shows a typical set of drying-rate data and the calculated values by the CDRC approach. For the overall drying rate vs. water content, the CDRC approach does not quite resemble the experimental trends.

Table 4. Drying Conditions That Were Used in Model Predictions under Time-Dependent Drying Conditions

Drying Air Initial Temperature (°C)	Drying Air Flow Rate (30 SLPM)	
	20 wt %	30 wt %
91.4	*, **	*, **
113.4	*, **	*, **

* Skim milk.
** Whole milk.

Table 5. Average Absolute Differences between the Experimental Data and Predictions by Either REA or CDRC Approach under Time-Dependent Drying Conditions

	Activation Energy		Characteristic Drying Curve	
	Temperature (°C)	Weight (%)	Temperature (°C)	Weight (%)
Skim milk	2.0	1.6	4.3	3.8
Whole milk	2.0	1.1	2.1	3.0

In the REA approach, the surface vapor concentration is estimated from the activation energy equation (such as Eq. 17). In any event, such a relationship is established using the experimental data. The vapor concentration at the interface of the droplet would be closely followed by the REA model for the constant drying conditions. The CDRC approach, on the other hand, assumes beforehand the drying behavior of the small droplets. However, it has been found that the REA approach does not necessarily exactly represent the initial drying/evaporation rate. Even at the high initial concentration (that is, 30 wt % used in this work), the first moment of the drying and the surface of the droplet would exhibit as if it were covered with pure water. This period is expected to be relatively short, which means the activation energy at this stage would better be represented as being zero. However, the values estimated from correlations (such as Eq. 23) obtained from the 20 and 30 wt % data were somewhat high (nonzero in any case). Thus, the predicted drying rates are expected to be smaller than reality. This may lead to a faster rise of the temperature of the droplet than predicted for the actual process of the initial drying stage (normally 10% of the total drying time as found in present study). Figure 11 shows an example of the milk droplet drying at the earliest stage. Because of the lower drying rates, in this figure, the temperatures of the droplets were overpredicted in the first 20 s. To further illustrate this drawback of the REA model, the following was conducted:

(1) Instead of directly using the master curve (Eq. 23), the

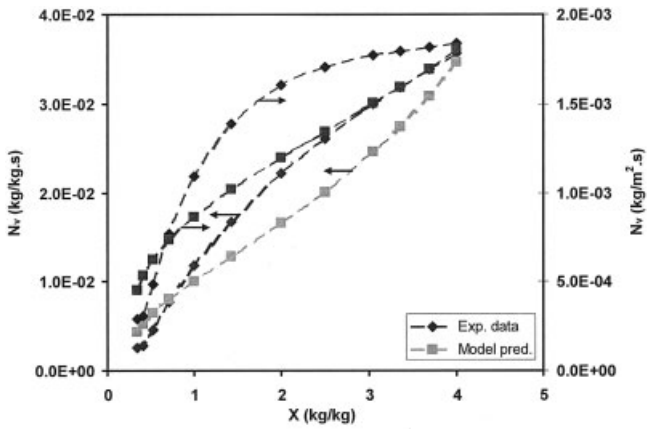

Figure 11. Comparison of the drying rate of the experimental data and predictions made using the CDRC model for 20 wt % skim milk under constant drying conditions.

T_b = 67.5 °C, v_b = 0.45 m/s, and H = 0.0001 kg/kg.

initial drying period may be approximated by the following equation, taken from Figure 12:

$$\frac{t}{d_0^2} = 18 \times 10^6 \qquad (\text{sec m}^{-2}) \tag{24}$$

Here, the normalized time variable t/d_0^2 was used, where t is the drying time and d_0 is the initial diameter of the droplet. Such normalization was suggested previously,[4,16] which enables direct comparison between droplets of different initial sizes, assuming the droplets have the same shape and the same solute diffusivities. Figure 12 shows the influence of the initial diameter on droplet diameter changes. From this figure, different milk droplet diameters vs. normalized time trends fall into the same curve but begin to deviate from the water curve when the normalized time passed 18×10^{-6} s m^{-2}. This is recognized as the "landmark " beyond which the drying follows the master curve defined by the REA approach. For a droplet with initial diameter of 1.45 mm for 30 wt %, for example, this period is 38 s. The water contents of the milk droplets after the corresponding initial periods can then be determined.

(2) After the above time period was determined, the value of the activation energy at the end of this period was calculated using Eq. 20 or 21. The initial value of the activation energy at time $t = 0$ is estimated at 1.2×105 J kmol^{-1} (this corresponds to 0.95 water activity). Other values between time $t = 0$ and the end of the low activation energy period were inserted linearly. Thus the modeling of the droplet drying was conducted again using this new varying activation energy for this initial period.

Through this correction, the difference between the predicted and the experimental results during the initial drying period is reduced. Figures 6 and 13 show such examples of predictions with and without the above correction, respectively. Figure 12 demonstrates the details of the drying during the first 20 s, in which the predicted results are better than those of Figure 11, which does not have the activation energy correction during the initial drying period.

Improvements of the REA model along the line suggested above may be possible. For example, when $t \leq 18 \times 10^6 \cdot d_0^2$, ΔE_v may be assumed to be zero. After that, the usual relationship of the REA model applies. The model fits may be improved overall. This is being tested together with other possible alternatives. Despite this, it is worthwhile noting that one can take the REA model as it is because it is already fairly accurate. It is noted here that, whether using the individual REA equation or the unified REA equation, the results are not much different among the data tested. On the other hand, there may also be room for improving the CDRC model by incorporating formulas that resemble to a greater degree the drying rate vs. moisture content relationship. In general, the REA model is preferred based on the results so far.

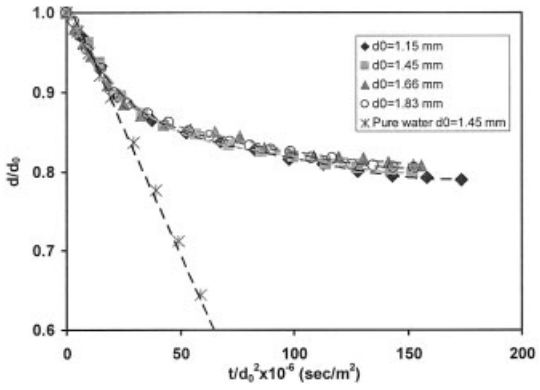

Figure 12. Influence of initial diameter on diameter change.

Whole milk, 30.0 wt % solids, $v_b = 0.45$ m s^{-1}, $T = 67.5$°C, $H = 0.0001$ kg/kg dry air.

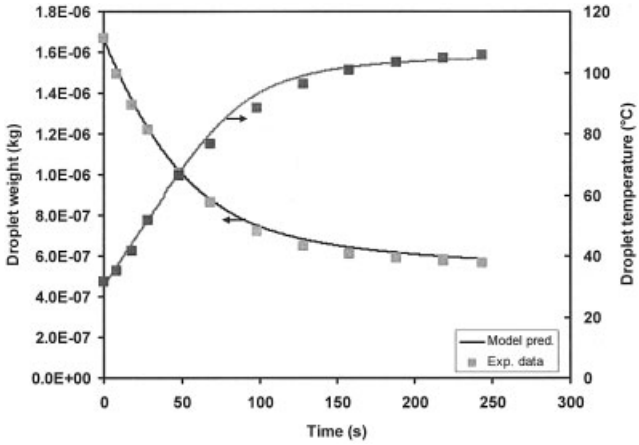

Figure 13. Comparison of the experimental data and predictions given by the REA model (with activation energy correction during initial drying period) for 30 wt % whole milk drying at T_b = 106.6°C, v_b = 0.45 m/s, and H = 0.0001 kg/kg.

Droplet initial weight = 1.668×10^{-6} kg. (This is a direct comparison with that in Figure 6.)

Conclusions

An improved glass-filament system for single-droplet drying studies was used herein to measure the drying kinetics under a wide range of constant and time-varying experimental conditions. The experimental results were much more extensive than those in previous studies. With these data, it was possible to validate both the CDRC approach and the REA approach. Both models predict the experimental results reasonably well. The REA model is better overall, although the REA approach has some drawbacks as indicated earlier in the discussion. The CDRC approach assumes beforehand the falling rate in all kinds of conditions for milk droplet drying, whereas the REA model simply reflects the experimental results closely. For the extreme conditions outside the range in the current work, greater differences may be expected between the two models. The REA model is experimentally based but its general nature requires very few experiments to obtain the model constants. Further work is being conducted using both models to predict the dryer-wide process to see whether the two models can predict similar profiles, especially to see whether the kind of accuracy of the model can affect food quality predictions. In particular, incorporation of the REA model into CFD modeling simulations[18-20] is of a high priority.

Notation

ΔE_v = apparent activation energy, J kmol^{-1}

ΔH_l = latent heat of water vaporization, J kg^{-1}
A = droplet surface area, m^2
a_w = water activity
Bi = Biot number
$C_{p,d}$ = specific heat capacity at constant pressure, J kg^{-1} K^{-1}
d = droplet diameter, m
f = relative drying rate
h = external heat transfer coefficient, W m^{-2} K^{-1}
h_m = external mass transfer coefficient, m s^{-1}
m = droplet mass, kg
m_o = monolayer moisture content, kg kg^{-1}
m_s = solid mass in one droplet/particle, kg
N_x = drying rate, kg kg^{-1} s^{-1}
$\dot{N}$ = drying rate in the first drying period, kg kg^{-1} s^{-1}
Nu = Nusselt number
Pr = Prandtl number
Re = Reynolds number
Sc = Schmidt number
Sh = Sherwood number
t = time, s
T_b = bulk air temperature, K
T_d = droplet temperature, K
T_s = surface temperature, K
T_{wb} = wet bulb temperature, K
X = average water content on dry basis, kg kg^{-1}
X_o = initial moisture content, kg kg^{-1}
X_b = equilibrium moisture content corresponding to the bulk (air) condition, kg kg^{-1}
X_{cr} = critical moisture content, kg kg^{-1}

Greek letters

ϕ = characteristic moisture content
ψ = fractionality coefficient or relative humidity at the interface of the droplet
ρ_v = vapor density, kg m^3

Subscripts

= initial value
b = bulk air
cr = critical value
d = dropler
l = latent heat
s = droplet surface
sat = saturation
v = vapor or vaporization
wb = web bulb

Literature Cited

1. Heldman DR, Lund DB. *Handbook of Food Engineering*. New York, NY: Marcel Dekker; 1992.
2. Rahman MdS. *Food Properties Handbook*. New York, NY: CRC Press; 1995.
3. Chen XD, Xie GZ. Fingerprints of the drying behavior of particulate or thin layer food materials established using a reaction engineering model. *Trans IChemE C*. 1997;75:213-222.
4. Lin SXQ, Chen XD. Improving the glass-filament method for accurate measurement of drying kinetics of liquid droplets. *Trans IChemE A*. 2002;80:401-410.
5. Sano Y, Keey RB. The drying of a spherical particle colloidal material into a hollow sphere. *Chem Eng Sci*. 1982;37:881-889.
6. Cheng HW, Jefferys GV, Mumford CJ. A receding interface model for the drying of slurry droplets. *AIChE J*. 1986;32:1334-1346.
7. Wijlhuizen AE, Kerkhof, PJAM, Bruin S. Theoretical study of inactivation of phosphatase during spray drying of skim-milk. *Chem Eng Sci*. 1979;34:651-660.
8. Langrish TAG, Kockel TK. The assessment of a characteristic drying curve for milk powder for use in computational fluid dynamics modeling. *Chem Eng J*. 2001;84:69-74.
9. Chen XD, Pirini W, Ozilgen M. The reaction engineering approach to modelling drying of thin layer of pulped kiwifruit flesh under conditions of small Biot numbers. *Chem Eng Prog*. 2001;40:165-181.
10. Ranz WE, Marshall WR. Evaporation from drops. *Chem Eng Process*. 1952;48:141-146, 173-178.
11. Downing CG. The evaporation of drops of pure liquids at elevated temperatures: Rate of evaporation and wet-bulb temperatures. *AIChE J*. 1966;12:760-766.
12. Chen XD, Reid D, Chen NX, Fletcher A, Pearce D. A new model for the drying of milk droplets for fast computation purposes. Proc of Chemeca'99 (on CD-ROM), Newcastle, Australia; 1999.
13. Chen XD. Lower bound estimate of the mass transfer coefficient of droplet evaporation-effect high mass flux. *Drying Technol*. 2005;23(1-2), 59-69.
14. Lin SXQ, Chen XD. Desorption isotherm of milk powders at elevated temperatures and over a wide relative humidity range. *J Food Eng*. 2003;00:000-000.
15. Chen XD, Peng XF. Modified Biot number analysis in the context of air drying. *Drying Technol*. 2005;23(1-2), 83-103.
16. Incropera FP, De Wit DP. *Fundamentals of Heat and Mass Transfer*. 3rd Edition. New York, NY: Wiley; 1990:216.
17. Lin SXQ, Chen XD. Changes in milk droplet diameter during drying under constant drying conditions investigated using the glass-filament method. *Trans IChemE C*. 2003;82(C3):213-218.
18. Langrish TAG, Zbincinski I. The effects of air inlet geometry and spray cone angle on wall deposition rate in spray dryers. *Trans IChemE*. 1994;72(A):420-430.
19. Huang L Mujumdar AS. A parametric study of the gas flow patterns and drying performance of co-current spray dryer: Results of a computational fluid dynamic study. *Drying Technol*. 2003;21:957-978.
20. Huang L, Kumar K, Mujumdar AS. Computational fluid dynamics simulation of droplet drying in a spray dryer. In: Silva MA, Rocha SCS, eds. *Proceedings of the 14th International Symposium* (*IDS 2004*)*—Drying 2004*. Vol. A. Sao Paulo, Brazil; 2004:326-327.

Manuscript received Mar. 1, 2004, and revision received Oct. 15, 2004.